2022

Impact of Cycle Parameters on Moisture Removal Rate of a Sorption-based Dehumidification System

Behnam Ahmadi

Masoud Ahmadi

Kashif Nawaz

Kyle Gluesenkamp

Sajjad Bigham

Impact of Cycle Parameters on Moisture Removal Rate of a Sorption-based Dehumidification System

Behnam AHMADI[1], Masoud AHMADI[2], Kashif NAWAZ[3], Kyle R. GLUSENKAMP[4], Sajjad BIGHAM[5]*

[1]Michigan Technological University, Department of Mechanical Engineering, Houghton, MI, USA
bahmadi@mtu.edu

[2]Michigan Technological University, Department of Mechanical Engineering, Houghton, MI, USA
masoudah@mtu.edu

[3]Oak Ridge National Laboratory, Building Equipment Research Group, Oak Ridge, TN, USA
nawazk@ornl.gov

[4]Oak Ridge National Laboratory, Building Equipment Research Group, Oak Ridge, TN, USA
glusenkampk@ornl.gov

[5]Michigan Technological University, Department of Mechanical Engineering, Houghton, MI, USA
sbigham@mtu.edu

* Corresponding Author

ABSTRACT

Effective moisture management is crucial to developing energy-efficient air conditioning systems, particularly at high latent cooling loads. Standard dehumidification systems rely on a low-temperature condensation process to dehumidify a humid air stream. This is an energy-intensive process due to a strong coupling between the sensible and latent cooling loads. Liquid sorption-based dehumidification cycles separate sensible and latent cooling loads by directly capturing humidity, thereby improving the overall energy efficiency of air conditioning systems. The moisture removal rate and energy performance of a liquid sorption-based dehumidification cycle highly depend on cycle parameters including desiccant flow rate and temperature of the desorption process. In this work, an advanced liquid-sorption-based dehumidification cycle is developed to investigate the impact of cycle operating parameters on the moisture removal rate at high moisture contents. Two desorption temperatures of 120 and 140°C and four liquid desiccant flow rates of 2.5, 3, 3.5, and 4 g/s are studied. Experimental results indicated that the moisture removal rate increases with the solution flow rate due to a boost in the effective desiccant-air interfacial area available for the dehumidification process. A maximum moisture removal rate of 0.1 g/s at a solution flow rate of 2.5 g/s and a desorber temperature of 140°C was measured. The knowledge developed from the present study expedites the development of energy-efficient sorption-based air conditioning systems enabling effective and independent moisture management.

1. INTRODUCTION

It is estimated that energy demand for space cooling will account for 37% of the global electricity consumption in 2050 (International Energy Agency (IEA), 2018). International Energy Agency (IEA) projects that the worldwide energy demand for space cooling could be reduced by as much as 45% if the energy efficiency of existing air conditioning (AC) systems doubles (International Energy Agency (IEA), 2018). A substantial share of the total energy consumption for space cooling is associated with the latent cooling load (Harriman et al., 1999). Although techno-economically mature, vapor compression cycle (VCC) based AC systems inefficiently handle the latent cooling load.

Particularly, the VCC-based AC systems need to operate below the dew point temperature to remove water vapor molecules from a humid air stream. The low operating temperature of the VCC system deteriorates the AC energy efficiency, especially in a humid climate (Ma & Horton, 2020). Therefore, the development of high-performance AC systems with effective latent load management is necessary to reduce the growing energy demand for space cooling.

Separate sensible and latent cooling (SSLC) AC systems are envisioned to be an alternative to conventional VCC-based AC systems. The SSLC systems manage the latent and sensible loads separately, thereby offering independent control over humidity (Ahmadi et al., 2021; Puttur et al., 2022). Gluesenkamp and Nawaz (Gluesenkamp & Nawaz, 2021) reported that the SSLC systems could reduce space-cooling energy consumption by 14 to 47% compared to conventional air conditioning systems. One strategy to separate sensible and latent loads is to utilize two evaporators operating at two different temperatures. In this approach, the low-temperature evaporator manages the latent load and the high-temperature evaporator is responsible for the sensible load (Ling et al., 2010). Although this arrangement reduces space-cooling energy consumption due to an increase in the evaporation temperature, it still relies on energy-hungry vapor compressors (Li et al., 2021).

Alternatively, a VCC system integrated with a desiccant system has the potential to further reduce the energy demand for space cooling. These systems manage sensible and latent loads separately at which the desiccant and VCC units handle the latent and sensible cooling loads, respectively (Nawaz & Gluesenkamp, 2018; Woods, 2014). Solid desiccant-based dehumidification technologies including desiccant wheels (DW) (Ali et al., 2022), packed desiccant beds (Yeboah & Darkwa, 2016), and fluidized beds (Chiang et al., 2016) are considered for SSLC-based air conditioning systems. Jia et al. (2006) experimentally evaluated the performance of a VCC unit integrated with a solid desiccant wheel. They observed the hybrid desiccant-VCC air conditioning system resulted in 37.5% energy saving compared with the conventional VCC systems (Jia et al., 2006). The desiccant-coated heat exchanger (DCHX) concept is another approach to managing high humidity loads. Here, a conventional heat exchanger is coated with solid desiccant materials. Tue et al. (2017), for example, coated the evaporator and condenser modules of a VCC unit with mesoporous silica gel powders. The solid-desiccant-coated modules directly capturing/releasing water vapor molecules resulted in a high electrical coefficient of performance of 7 (Tu et al., 2017). Despite their ease of use, existing solid-desiccant-based systems suffer from several drawbacks including high air-side pressure drop penalties, high regeneration temperatures, and the formation of fine dust particles in the supply air stream (Misha et al., 2012).

A liquid-desiccant-based dehumidification system could address several shortcomings of a solid-desiccant-based system. Particularly, liquid-desiccant-based dehumidification systems offer high moisture removal rates and energy efficiency metrics (Bigham, Yu, et al., 2014; Mortazavi et al., 2015; Nasr Isfahani et al., 2015). Additionally, liquid-desiccant-based systems require a low-temperature regeneration process, thereby allowing utilization of low-grade energy sources including solar energy (Bigham, Nasr Isfahani, et al., 2014; Mohammad et al., 2016) or potentially waste heat of a condenser unit. Bergero and Chiari (2011) analyzed the performance of a hybrid liquid-desiccant-VCC system. They reported a 60% energy saving at high latent cooling loads (Bergero & Chiari, 2011). Mansuriya et al. (2020) combined a liquid-desiccant dehumidification system with a VCC unit to independently control the latent cooling load in a hot and humid climate. Their experimental results showed a 27.5% improvement in the coefficient of performance of the hybrid system compared to a standalone VCC unit (Mansuriya et al., 2020).

In a liquid desiccant-based air conditioning system, cycle parameters play an important role in the overall performance. In this study, a well-equipped lithium-bromide-based dehumidification cycle is developed to examine the effects of the liquid desiccant flow rate and operating temperature of the desorber module on the moisture removal rate and energy performance under hot and humid climate conditions. In the following sections, first, the design and development of the dehumidification test facility including the dehumidifier and desorber modules are discussed. Next, data reduction and test procedures are discussed in detail. Finally, the effects of different solution flow rates and temperatures of the desorber module on the dehumidification rate and energy performance of the system are experimentally investigated.

2. EXPERIMENT AND UNCERTAINTY ANALYSIS

2.1 Sorption-based Dehumidification Test Facility

A liquid-desiccant-based dehumidification test facility was developed to experimentally evaluate the impact of sorption-cycle parameters including desorber solution flow rate and temperature on moisture removal rate. Fig. 1

shows a schematic of the experimental test setup. The sorption-based dehumidification test facility consists of a liquid-desiccant-based dehumidifier module, a desorber module, a solution heat exchanger, an oil heat exchanger, an air flow meter, and two Coriolis solution mass flow meters (Model: Emerson Electric Co., Micro Motion Elite Coriolis Flow/Density Meter, CMFS series). The two Coriolis solution mass flow meters monitor the temperature, density, and flow rate of the lithium bromide (LiBr) solution entering and leaving the dehumidifier module. First, a strong LiBr solution flows over the dehumidifier module. Here, the strong LiBr solution absorbs water vapor molecules from a humid air stream and becomes a water-rich weak LiBr solution. The difference in the water vapor pressure potential between the air and LiBr solution drives the dehumidification process. The weak LiBr solution is then pre-heated in a solution heat exchanger before entering the desorber module. As shown in the zoomed inset image in Fig. 1, the thermal energy supplied by the oil heat exchanger rejects the initially-captured water vapor molecules from the weak LiBr solution. The desorbed water vapor molecules are dumped into the outside ambient. The strong and hot LiBr then passes through the solution heat exchanger and then flows back to the dehumidifier module to complete the LiBr solution loop. The solution heat exchanger between the dehumidifier and desorber modules plays a significant role in recuperating the sensible thermal energy of the desorber module, thus improving the overall energy efficiency of the sorption-based dehumidification process.

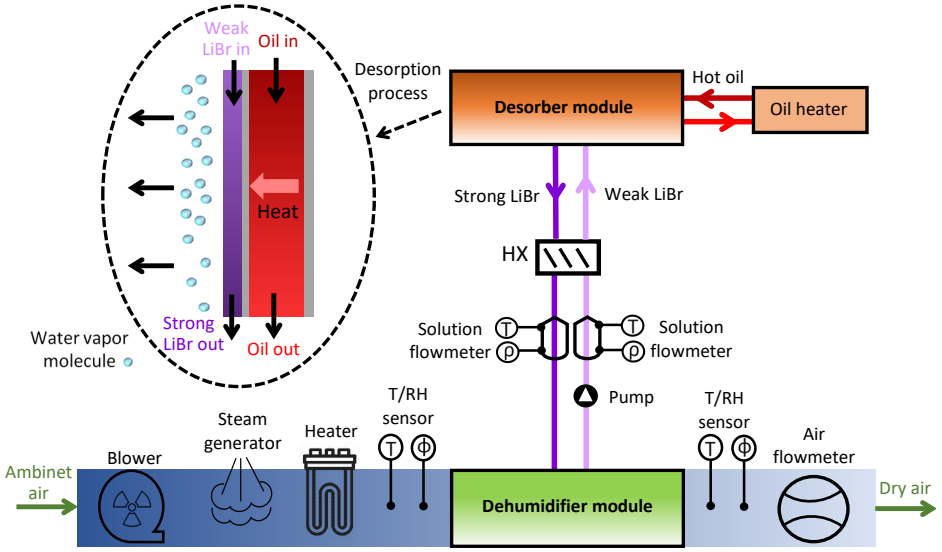

Figure 1: A schematic of the sorption-based dehumidification test facility. HX, T, and RH stand for heat exchanger, temperature, and relative humidity, respectively.

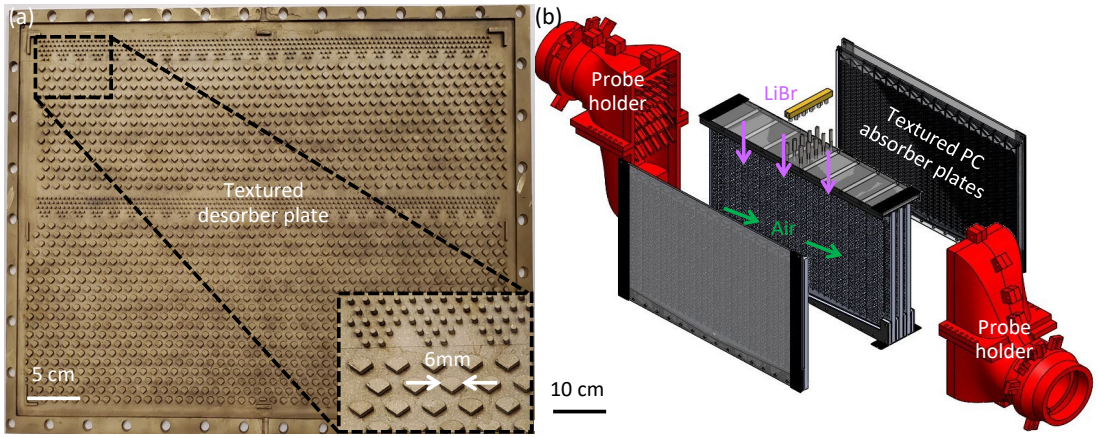

Figure 2: (a) An image of the desorber plate employing brass textures for better flow distribution, and (b) a schematic of the dehumidifier module.

The air loop includes an air blower, a mist generator, an air heater, a honeycomb laminated air flow meter (Model: Air Monitor Inc., 4" LO-flo/P with an integral temperature probe), and temperature and relative humidity sensors (Model: Vaisala Inc., HMT 337). The mist generator and air heater units supply an air stream with the desired temperature and relative humidity to the dehumidifier module. In the dehumidifier module, the strong LiBr solution captures the humidity of the warm and humid air stream. It should be mentioned that the thermo-hydraulic properties of both LiBr solution and air stream are measured and controlled at various locations to better analyze the heat and mass transfer performance of each module under different operating conditions.

Fig. 2a shows an image of the desorber plate made of brass. The overall size of the desorber plate is 30.5 × 405.7 cm^2 with a thickness of 6.35 mm. The drop-shaped textures with a height of 2 mm and an edge-to-edge spacing of 6 mm were created to enhance the LiBr flow distribution onto the desorber plate. Fig. 2b shows an exploded view of the dehumidifier module. The dehumidifier module includes five double-sided textured polycarbonate plates, a solution distributor, two cover plates, and two 3D-printed air manifolds. Each dehumidifier plate has a thickness of 6.35 mm and a surface area of 30.5 × 45.7 cm^2.

2.2 Data reduction and uncertainty analysis

Nominal values, ranges, experimental errors, and uncertainties of the main test parameters including solution flow rate, solution density, solution temperature, air flow rate, air relative humidity, air temperature, and oil temperature are listed in Table 1. The moisture removal rate per projected area of the dehumidifier surface is defined as the dehumidification rate, J_{deh}, as follow:

$$J_{deh} = \frac{\dot{m}_{air}(\omega_{air,in}-\omega_{air,out})}{A_{proj}} = \frac{\dot{m}_{LiBr}(x_{LiBr,in}-x_{LiBr,out})}{A_{proj}}, x_{LiBr} = f(T_{LiBr}, \rho_{LiBr}) \quad (1)$$

where $\dot{m}_{air}$ is air mass flow rate, ω_{air} is humidity ratio of the air, $\dot{m}_{LiBr}$ is the LiBr solution mass flow rate, x_{LiBr} is the LiBr solution concentration which is a function of temperature T_{LiBr} and density ρ_{LiBr}, and A_{proj} is the total projected area. The total projected area of the dehumidifier module with ten absorber plates is 1 m^2. The dehumidification rate is equal to the amount of the desorbed water molecules from the solution in the desorber module (i.e., desorption rate). The uncertainty associated with the dehumidification rate (J_{deh}) is calculated using the following equation:

$$\frac{\delta J_{deh}}{J_{deh}} = \sqrt{\left(\frac{\delta \dot{m}_{LiBr}}{\dot{m}_{LiBr}}\right)^2 + 2\left(\frac{\delta \rho_{LiBr}}{\rho_{LiBr}}\right)^2 + 2\left(\frac{\delta T_{LiBr}}{T_{LiBr}}\right)^2} \quad (2)$$

The moisture removal rate in the dehumidifier module is a function of the water vapor pressure potential (ΔP) between the inlet humid air and LiBr solution as follows:

$$\Delta P = P_{wv,air,in}(T_{air}, \phi_{air}) - P_{wv,LiBr,in}(T_{LiBr}, x_{LiBr}) \quad (3)$$

where $P_{wv,air}$, the partial water vapor pressure of the air, is a function of air temperature T_{air} and relative humidity ϕ_{air}, and $P_{wv,LiBr}$ is the equilibrium water vapor pressure of the LiBr solution. The overall thermal efficiency of the system (η) representing the system performance can be determined as follow:

$$\eta = \frac{\dot{m}_{air}(\omega_{air,in} - \omega_{air,out})h_{fg}}{\dot{Q}_{net,des}} \quad (4)$$

where h_{fg} is the latent heat of evaporation, and $\dot{Q}_{net,des}$ is the net input thermal energy provided by the hot oil to the desorber module. The uncertainty associated with system thermal efficiency and the net thermal energy input can be estimated as follows:

$$\frac{\delta\eta}{\eta} = \sqrt{\left(\frac{\delta\dot{m}_{air}}{\dot{m}_{air}}\right)^2 + \left(\frac{\delta\omega_{air,in}}{\omega_{air,in}}\right)^2 + \left(\frac{\delta\omega_{air,out}}{\omega_{air,out}}\right)^2 + \left(\frac{\delta\dot{Q}_{net,des}}{\dot{Q}_{net,des}}\right)^2} \quad (5)$$

$$\frac{\delta\dot{Q}_{net,des}}{\dot{Q}_{net,des}} = \sqrt{\left(\frac{\delta\dot{m}_{LiBr}}{\dot{m}_{LiBr}}\right)^2 + 2\left(\frac{\delta T_{LiBr}}{T_{LiBr}}\right)^2 + \left(\frac{\delta\dot{m}_v}{\dot{m}_v}\right)^2} \quad (6)$$

where $\dot{m}_v$ is the vapor generation rate (i.e., desorption rate) defined as:

$$\dot{m}_v = \dot{m}_{LiBr}(x_{out,des} - x_{in,des}) \quad (7)$$

The uncertainty associated with the vapor generation rate is defined as follow:

$$\frac{\delta\dot{m}_v}{\dot{m}_v} = \sqrt{\left(\frac{\delta\dot{m}_{LiBr}}{\dot{m}_{LiBr}}\right)^2 + 2\left(\frac{\delta T_{LiBr}}{T_{LiBr}}\right)^2 + 2\left(\frac{\delta\rho_{LiBr}}{\rho_{LiBr}}\right)^2} \quad (8)$$

Table 1: Nominal values, ranges, experimental errors, and uncertainties of the main test parameters.

Parameter [unit]	Nominal value	Range	Experimental error	Uncertainty
LiBr solution flow rate [g/s]	3.25	2.5 - 4	± 0.325	± 0.1 %
LiBr solution density [kg/m^3]	1450	1445 - 1455	± 0.5	± 0.03 %
LiBr solution temperature [°C]	40	38 - 42	± 1	± 2.5 %
Air volumetric flow rate [CFM]	100	95 - 105	± 2.4	± 2.4 %
Relative humidity [%]	80	78 - 82	± 1	± 1.25 %
Air temperature [°C]	32.5	32-33	± 0.2	± 0.6 %
Humidity ratio [$g_{water}/kg_{dry\text{-}air}$]	24.8	23.8 – 25.8	± 2.5	± 5 %
Oil flow rate [g/s]	50	48 - 52	± 0.5	± 1 %
Oil temperature [°C]	130	120 - 140	± 1	± 0.8 %
Desorber heat input [W]	600	400 - 800	± 28	± 4.6 %

2.3 Test procedure

The performance of the proposed sorption-based dehumidification system was experimentally examined at different desorber operating temperatures (i.e., inlet oil temperatures) and desorber solution mass flow rates. First, the solution mass flow rate of the desorber module was adjusted to the desired value. Five different desorber mass flow rates of 2.5, 3, 3.5, and 4 g/s were examined. Then, the air flow rate was set to 56.86 m^3/h (i.e., 100 CFM). Next, the mist generator and the electric heater were adjusted to deliver an air stream with a temperature and relative humidity of 32.5 °C and 80% to the dehumidifier module, respectively. Finally, the oil heater was adjusted to supply a target inlet oil temperature (i.e., 120 or 140°C) to the desorber module.

During each test, the desorber inlet solution mass flow rate and concentration, dehumidifier inlet air temperature, dehumidifier inlet air relative humidity, and inlet hot oil temperature were continuously monitored to ensure a steady-state operating condition. The temperature and density of the LiBr solution were measured by the two Coriolis solution mass flow meters at the inlet/outlet of the dehumidifier module. The concentration of LiBr solution at the inlet of the desorber module was fixed at 45%. The relative humidity and temperature of the air flow stream were monitored by humidity sensors and thermocouples positioned at the inlet/outlet of the dehumidifier module. Additionally, the temperatures of the inlet/outlet hot oil stream were monitored by two thermocouples at the inlet/outlet oil heat exchanger. Each experimental data point was allowed at least 30 min to reach a steady-state operating at which there

was no continuous rise and/or decline in operating parameters. Furthermore, each test was repeated at least three times to ensure the repeatability of the data presented.

3. RESULTS AND DISCUSSION

Fig. 3a shows the humidity ratio of the dehumidifier outlet air as a function of desorber solution flow rate at two different inlet oil temperatures of 120 and 140°C. The dehumidifier inlet air has a temperature of 32.5°C, relative humidity of 80%, and a humidity ratio of 25.33 $g_{water}/kg_{dry\text{-}air}$. Here, the strong LiBr solution absorbs the water vapor molecules of the humid air flow stream, thereby reducing the humidity ratio of the dehumidifier air outlet. As shown, the dehumidifier outlet air humidity ratio increases with the desorber LiBr solution mass flow rate. For example, at a desorber operating temperature of 140°C, the dehumidifier outlet air humidity ratio increases from 23.4 to 23.8 $g_{water}/kg_{dry\text{-}air}$ when the desorber LiBr flow rate increases from 2.5 to 4 g/s. Increasing the desorber LiBr flow rate results in a thicker solution film over the desorber plate, thereby reducing the desorption rate. At a lower desorption rate, the concentration of the LiBr solution leaving the desorber module and entering the dehumidifier module is low. A LiBr solution with a lower concentration has a weaker affinity to absorb water vapor molecules of the humid air stream. Hence, the dehumidifier outlet air humidity ratio increases at higher desorber LiBr flow rates. This is consistent with Fig. 3b which shows the moisture removal rate of the dehumidifier module decreases at higher desorber LiBr mass flow rates.

Fig. 3a also shows that the air leaving the dehumidifier module is drier at higher desorber LiBr temperatures. This is attributed to the desorber outlet LiBr concertation, which increases at higher desorber temperatures. At higher LiBr concentrations, the partial water vapor pressure potential of the dehumidification process increases, thereby improving the moisture removal rate as shown in Fig. 3b. A maximum moisture removal rate of 0.1 g/m^2-s was obtained at a desorber LiBr flow rate of 2.5 g/s and an inlet oil temperature of 140°C.

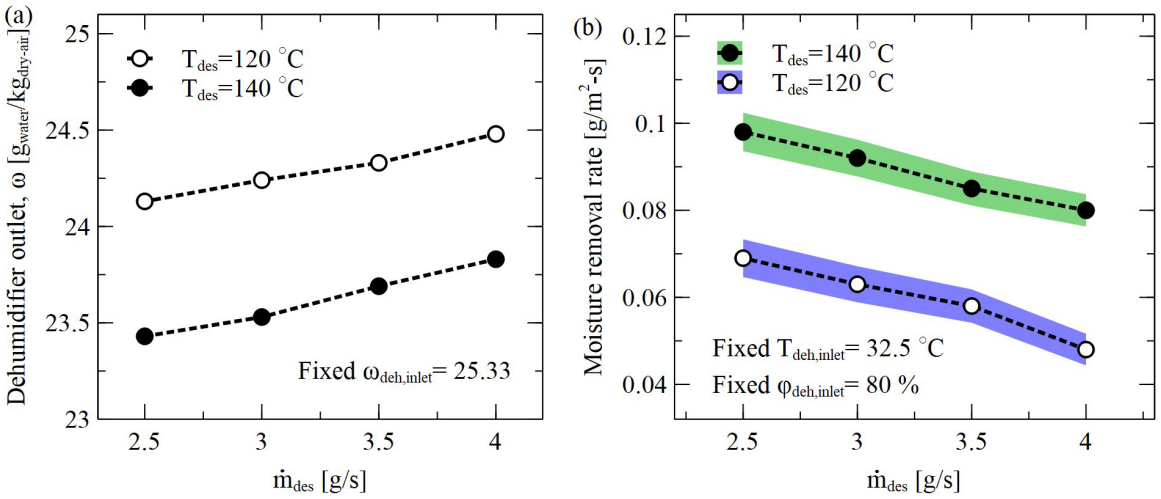

Figure 3: (a) Dehumidifier outlet air humidity ratio, and (b) moisture removal rate as a function of desorber LiBr solution mass flow rate at two inlet oil temperatures of 120 and 140°C.

To examine the effect of cycle parameters on system performance, the net thermal energy efficiency of the dehumidification process was studied at different desorber solution flow rates and two inlet oil temperatures of 120 and 140°C. As shown in Fig. 4, the net thermal energy efficiency of the system increases at higher inlet oil temperatures. For example, at a desorber solution flow rate of 4 g/s, the energy efficiency improves from 20 to 28% when the inlet oil temperature increases from 120 to 140°C. This is attributed to the desorption process, which becomes more energy efficient at higher temperatures. Additionally, for a given inlet oil temperature, the system energy efficiency is improved as the solution flow rate decreases. This is because a larger part of the input thermal energy is utilized for the phase-change regeneration process than the sensible heating of the LiBr solution. At a solution flow rate of 2.5 g/s and inlet oil temperature of 140°C, a maximum thermal energy efficiency of 35% was obtained.

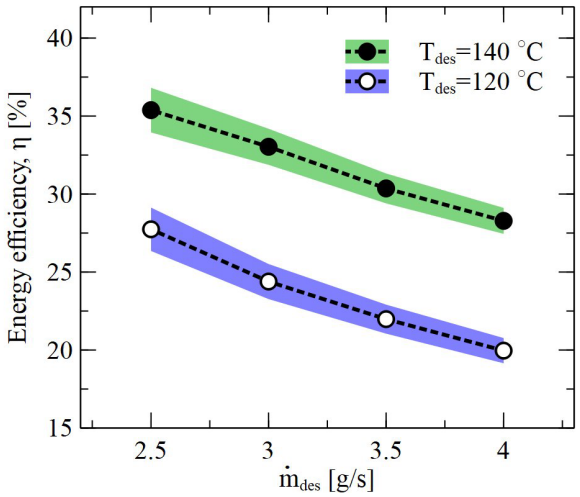

Figure 4: Variations of system thermal energy efficiency as a function of desorber LiBr solution mass flow rate at two inlet oil temperatures of 120 and 140°C.

4. CONCLUSIONS

This study experimentally investigated the moisture removal rate and thermal energy efficiency of a liquid-desiccant-based dehumidification system at different desorber LiBr solution flow rates and temperatures. The results revealed that the moisture removal rate and system thermal efficiency decrease when the desorber LiBr solution flow rate increases. Additionally, the moisture removal rate and system thermal efficiency are improved at higher desorber temperatures. A maximum moisture removal rate of 0.1 g/s and a maximum thermal energy efficiency of 35% were realized at a solution flow rate of 2.5 g/s and a desorber temperature of 140°C. The results of the present study help to design future energy-efficient liquid-desiccant-based air conditioning systems.

NOMENCLATURE

AC	Air conditioning	(–)
IEA	International energy agency	(–)
VCC	Vapor compression cycle	(–)
SSLC	Separate sensible and latent cooling	(–)
SD	Solid desiccant	(–)
DW	Desiccant wheel	(–)
DCHX	Desiccant-coated heat exchanger	(–)
LD	Liquid desiccant	(–)
LiBr	Lithium bromide	(–)
J	Dehumidification rate	(g/s-m^2)
$P_{wv,air}$	Partial water vapor pressure of the airside	(kPa)
$P_{wv,LiBr}$	Partial water vapor pressure of the LiBr solution	(kPa)
T	Temperature	(°C)
v	Vapor	(–)
x	Solution concentration	(%)
$\dot{m}$	Mass flow rate	(g/s)
h_{fg}	Latent heat of vaporization	(kJ/kg)

$\dot{Q}$	Net heat input	(kW)
ω	Humidity ratio	$g_{water}/kg_{dry\text{-}air}$
η	Efficiency	%
ρ	Density	kg/m^3
δ	Uncertainty	(–)
ϕ	Relative humidity	(%)
Subscript		
deh	Dehumidification	(–)
des	Desorber	(–)
in	Inlet	(–)
out	Outlet	(–)

ACKNOWLEDGEMENT

This study was sponsored by the US Department of Energy's Office of Energy Efficiency and Renewable Energy (EERE) under the Building Technology Office Award Number DEEE0008685. The authors would like to acknowledge Mr. Antonio Bouza and Mr. Mohammed Khan, Technology Managers, and Mr. Andrew Kobusch, Project Engineer, HVAC, Water Heating, and Appliance subprogram, Building Technologies Office, US Department of Energy.

REFERENCES

Ahmadi, B., Ahmadi, M., Nawaz, K., Momen, A. M., & Bigham, S. (2021). Performance Analysis and Limiting Parameters of Cross-flow Membrane-based Liquid-desiccant Air Dehumidifiers. *International Journal of Refrigeration*, *132*(September), 21–29. https://doi.org/10.1016/j.ijrefrig.2021.09.010

Ali, M., Habib, M. F., Ahmed Sheikh, N., Akhter, J., & Gilani, S. I. ul H. (2022). Experimental investigation of an integrated absorption- solid desiccant air conditioning system. *Applied Thermal Engineering*, *203*(August 2021), 117912. https://doi.org/10.1016/j.applthermaleng.2021.117912

Bergero, S., & Chiari, A. (2011). On the performances of a hybrid air-conditioning system in different climatic conditions. *Energy*, *36*(8), 5261–5273. https://doi.org/10.1016/j.energy.2011.06.030

Bigham, S., Nasr Isfahani, R., & Moghaddam, S. (2014). Direct molecular diffusion and micro-mixing for rapid dewatering of LiBr solution. *Applied Thermal Engineering*, *64*(1–2), 371–375. https://doi.org/10.1016/j.applthermaleng.2013.12.031

Bigham, S., Yu, D., Chugh, D., & Moghaddam, S. (2014). Moving beyond the limits of mass transport in liquid absorbent microfilms through the implementation of surface-induced vortices. *Energy*, *65*, 621–630. https://doi.org/10.1016/j.energy.2013.11.068

Chiang, Y. C., Chen, C. H., Chiang, Y. C., & Chen, S. L. (2016). Circulating inclined fluidized beds with application for desiccant dehumidification systems. *Applied Energy*, *175*, 199–211. https://doi.org/10.1016/j.apenergy.2016.05.009

Gluesenkamp, K. R., & Nawaz, K. (2021). Separate sensible and latent cooling: Carnot limits and system taxonomy. *International Journal of Refrigeration*, *127*, 128–136. https://doi.org/10.1016/j.ijrefrig.2021.02.019

Harriman, L. G., Plager, D., & Kosar, D. (1999). Dehumidification and cooling loads from ventilation air. *Energy Engineering: Journal of the Association of Energy Engineering*, *96*(6), 31–45. https://doi.org/10.1080/01998595.1999.10530479

International Energy Agency (IEA). (2018). *"The Future of Cooling Opportunities for energy- efficient air conditioning"International Energy Agency Website: www.iea.org, 2018*. www.iea.org

Jia, C. X., Dai, Y. J., Wu, J. Y., & Wang, R. Z. (2006). Analysis on a hybrid desiccant air-conditioning system. *Applied Thermal Engineering*, *26*(17–18), 2393–2400. https://doi.org/10.1016/j.applthermaleng.2006.02.016

Li, Z., Gluesenkamp, K. R., & Nawaz, K. (2021). Analysis of basic airflow configurations for separate sensible and latent cooling systems with indoor air recirculation. *International Journal of Refrigeration*, *127*, 78–88. https://doi.org/10.1016/j.ijrefrig.2020.12.026

Ling, J., Hwang, Y., & Radermacher, R. (2010). Theoretical study on separate sensible and latent cooling air-conditioning system. *International Journal of Refrigeration*, *33*(3), 510–520. https://doi.org/10.1016/j.ijrefrig.2009.11.011

Ma, J., & Horton, W. T. (2020). A sequential approach for achieving separate sensible and latent cooling. *International Journal of Refrigeration*, *117*, 104–113. https://doi.org/10.1016/j.ijrefrig.2020.04.004

Mansuriya, K., Raja, B. D., & Patel, V. K. (2020). Experimental assessment of a small scale hybrid liquid desiccant dehumidification incorporated vapor compression refrigeration system: An energy saving approach. *Applied Thermal Engineering*, *174*(November 2019), 115288. https://doi.org/10.1016/j.applthermaleng.2020.115288

Misha, S., Mat, S., Ruslan, M. H., & Sopian, K. (2012). Review of solid/liquid desiccant in the drying applications and its regeneration methods. *Renewable and Sustainable Energy Reviews*, *16*(7), 4686–4707. https://doi.org/10.1016/j.rser.2012.04.041

Mohammad, A. T., Mat, S. Bin, Sopian, K., & Al-Abidi, A. A. (2016). Review: Survey of the control strategy of liquid desiccant systems. *Renewable and Sustainable Energy Reviews*, *58*, 250–258. https://doi.org/10.1016/j.rser.2015.12.333

Mortazavi, M., Nasr Isfahani, R., Bigham, S., & Moghaddam, S. (2015). Absorption characteristics of falling film LiBr (lithium bromide) solution over a finned structure. *Energy*, *87*, 270–278. https://doi.org/10.1016/j.energy.2015.04.074

Nasr Isfahani, R., Bigham, S., Mortazavi, M., Wei, X., & Moghaddam, S. (2015). Impact of micromixing on performance of a membrane-based absorber. *Energy*, *90*, 997–1004. https://doi.org/10.1016/j.energy.2015.08.006

Nawaz, K., & Gluesenkamp, K. (2018). *Separate sensible and latent cooling systems : A critical review of the state-of-the-art and future prospects*.

Puttur, U., Ahmadi, M., Ahmadi, B., & Bigham, S. (2022). A novel lung-inspired 3D-printed desiccant-coated heat exchanger for high-performance humidity management in buildings. *Energy Conversion and Management*, *252*(October 2021), 115074. https://doi.org/10.1016/j.enconman.2021.115074

Tu, Y. D., Wang, R. Z., Ge, T. S., & Zheng, X. (2017). Comfortable, high-efficiency heat pump with desiccant-coated, water-sorbing heat exchangers. *Scientific Reports*, *7*(October 2016), 1–10. https://doi.org/10.1038/srep40437

Woods, J. (2014). Membrane processes for heating, ventilation, and air conditioning. *Renewable and Sustainable Energy Reviews*, *33*, 290–304. https://doi.org/10.1016/j.rser.2014.01.092

Yeboah, S. K., & Darkwa, J. (2016). A critical review of thermal enhancement of packed beds for water vapour adsorption. *Renewable and Sustainable Energy Reviews*, *58*, 1500–1520. https://doi.org/10.1016/j.rser.2015.12.134